IEEE Access
Multidisciplinary | Rapid Review | Open Access Journal

Received June 14, 2020, accepted June 19, 2020, date of publication June 22, 2020, date of current version July 1, 2020.

Digital Object Identifier 10.1109/ACCESS.2020.3004202

Parametric Reconstruction Method for the Long Time-Series Return-Stroke Current of Triggered Lightning Based on the Particle Swarm Optimization Algorithm

XIANGPENG FAN[1,2,3], WEN YAO[1], YANG ZHANG[1], LIANGTAO XU[1], YIJUN ZHANG[2], PAUL R. KREHBIEL[3], DONG ZHENG[1], HENGYI LIU[1], WEITAO LYU[1], SHAODONG CHEN[4], (Member, IEEE), AND ZHENGSHUAI XIE[1]

[1]State Key Laboratory of Severe Weather (LASW), Chinese Academy of Meteorological Sciences, Beijing 100081, China
[2]Department of Atmospheric and Oceanic Sciences, Institute of Atmospheric Sciences, and CMA-FDU Joint Laboratory of Marine Meteorology, Shanghai 200438, China
[3]Langmuir Laboratory for Atmospheric Research, Geophysical Research Center, New Mexico Institute of Mining and Technology, Socorro, NM 87801, USA
[4]Guangdong Provincial Key Laboratory of Regional Numerical Weather Prediction, Guangzhou Institute of Tropical and Marine Meteorology, China Meteorological Administration, Guangzhou 510080, China

Corresponding author: Yijun Zhang (zhangyijun@fudan.edu.cn)

This work was supported in part by the National Key Research and Development Program of China under Grant 2019YFC1510103, in part by the National Natural Science Foundation of China under Grant 41875001, Grant 41775009, and Grant 41775007, in part by the Basic Research Fund of the Chinese Academy of Meteorological Sciences under Grant 2018Z003 and Grant 2020Z009, and in part by the National Science Foundation under Grant AGS 1720600.

ABSTRACT The lightning research group of the Chinese Academy of Meteorological Sciences has carried out observations and experiments with artificially triggered lightning for more than ten years, and it accumulated thousands of examples of channel base current data on the return stroke of artificially triggered lightning prior to 2020. Based on the current data, this paper explores ways of improving the constructed function of a long time-series (400 μs) return stroke and the parametric reconstruction of the current waveform. The long time-series current can be divided into three components: the breakdown pulse current, corona current and quasi-uniform current. The corona current and quasi-uniform current are constructed by a Heidler function, while the breakdown pulse current is determined by the waveform characteristics of the current peak, which can be divided into the Heidler type and high-order exponential type. According to the three-component model of the return-stroke current, a two-step parametric reconstruction method for the long time-series lightning return-stroke current based on the particle swarm optimization (PSO) algorithm is proposed. In this paper, the results of the parameterized reconstruction of 14 return strokes are given, and the results of the multidimensional error analysis of 13 long time-series return strokes are given to illustrate the accuracy of the improved parameterized model of the return-stroke current and the effectiveness of the two-step reconstruction method based on the PSO algorithm.

INDEX TERMS Artificially triggered lightning, channel base current, Heidler function, particle swarm optimization, return stroke.

I. INTRODUCTION

Lightning is a kind of strong electrical discharge in the atmosphere. The peak current in the lightning return stroke can reach tens or even hundreds of kA. The peak temperature of the lightning discharge channel can reach 30000 K, which is approximately five times the solar surface temperature [1]. It also develops very quickly, with the same speed order of light. This kind of fast, high-current discharge process heats the channel quickly, thus producing various physical effects, such as optical radiation, electrical radiation, magnetic radiation, and thermal radiation, and chemical effects [1].

The associate editor coordinating the review of this manuscript and approving it for publication was Sotirios Goudos.

Disasters caused by lightning are usually related to these effects. The thermal effects caused by a fast-strong current heats the air and causes a high temperature and pressure in the lightning channel, which may lead to damage to buildings, explosions of oil tanks in warehouses, human and animal casualties and other disastrous events. Many studies have also confirmed that during the propagation of lightning, the channel current increases the content of nitrogen oxides and ozone in the atmosphere [2]–[6]. The ''photoelectric, thermal, magnetic and chemical effects'' of lightning are fundamentally related to the current in the lightning channel, but in most cases, this current cannot be measured directly. The lightning channel current is the key in studying many kinds of atmospheric physical processes and phenomena related to lightning, but only in a few cases can the current of the lightning return stroke be measured directly, such as those of tower lightning and artificially triggered lightning. Therefore, it is of great importance to study and parameterize the lightning return stroke current obtained from these kinds of measurements; such study is helpful not only in understanding the characteristics of the physical process of lightning but also to the development of relevant models; and of course, it is of great reference value for various engineering applications.

Therefore, for a long time, constructing the lightning return stroke current accurately and parametrically has been an important research issue, and various function construction models for lightning currents have been developed [7]. Bruce and Golde [8] proposed modeling the channel base current with a double exponential function, which provided a model for the simulation, theoretical research and engineering applications of the lightning return stroke current in the early stages of study. However, the problem with the biexponential model is that its first derivative is not zero when $t = 0$, which is meaningless in physics and makes the function initially discontinuous [9]. At present, the most widely used lightning current model is the Heidler function proposed by Heidler [10], which has been recognized as an international standard (IEC 62305-1, 2010). Later, some studies found that, based on the Heidler function, two Heidler functions can be summed [11], [12], or a Heidler function can be summed with a double exponential function [13], which can better construct the return-stroke current of the ground flash to a certain extent. In addition, as early as the 1980s, Lin *et al.* [14] proposed a theoretical model of the return stroke process, which divides the return-stroke current into three components, namely, the breakdown pulse current, corona current and uniform current. Nucci *et al.* [13] modeled the return stroke current by summing a Heidler function and a double exponential function with a 3 kA uniform current. These continuous improvements and attempts aim to make the modeled channel base current closer to the measured current, and the purpose of combining different functions is to give the constructed current the local characteristics of the measured current.

However, it must be pointed out that there are some shortcomings in these current construction models. First, a single Heidler function cannot perfectly construct the current waveform, which is not exactly consistent with the measured lightning return stroke current in most cases. The current construction model, which sums two Heidler functions or one Heidler function and one exponential function, can reconstruct the current waveform accurately only on the time scale of a few microseconds to tens of microseconds, but in a long time scale (hundreds of microseconds or even thousands of microseconds), the error of the constructed current waveform will increase significantly, and it is found that this kind of construction error is usually larger for a strong return stroke with a peak current of tens of kA. In addition, it is of physical significance to add a uniform current when constructing the return-stroke current in some models, but this uniform current is in conflict with observed facts. These current construction methods have a certain accuracy in a short time series of tens of microseconds, but the current constructed in a long time series has a large error compared with the measured current, which limits the application scenarios of the constructed current and its corresponding parameters.

In addition, with the improvement of the reconstruction model of lightning return stroke current, different methods have been introduced into the calculation of return stroke current reconstruction parameters. Vujević *et al.* [15] proposed the least square method to estimate the parameters of the Heidler function. Lundengård *et al.* [16], [17] proposed the of Marquardt least square method to estimate the parameters of measured lightning current. Chandrasekaran and Punekar [18] proposed a method to determine the functional parameters of the lightning channel base current by using genetic algorithm (GA), and Liu *et al.* [19] presented the particle swarm optimization (PSO) method to identify the lightning channel base current function parameters. Recently, using the measured return stroke current data of artificially triggered lightning obtained by our research team, Yang *et al.* [20] applied the PSO algorithm to the calculation of the measured current reconstruction parameters of triggered lightning and reconstructed the channel base current waveform of a 40 μs, relatively short time-series with the parametric model of the sum of two Heidler functions. At the same time, Yang *et al.* [20] also compared the performance differences between PSO algorithm and GA algorithm in solving current parameters. The results show that the parameters of Heidler function evaluated by the PSO method can achieve more accurate values than the parameters evaluated by GA. Generally speaking, these parameter calculation methods can reconstruct the return stroke current waveform in a short time scale (usually tens of microseconds), but the accuracy of the reconstructed current is limited by the insufficiency of the reconstruction model.

Therefore, based on the observation and analysis of a large number of measured channel base-current waveform characteristics of artificially triggered lightning, this paper improves the constructor of the channel base current based on the Heidler function. The improved return stroke current model is more complete and can accurately construct the return stroke

current waveform on a long-time scale (up to 400 μs, far more than the current reconstruction ability only in tens of microseconds). However, since the number of parameters in the improved model reaches 12-14, the PSO algorithm cannot be used to obtain the parameter values directly. Therefore, this paper proposes a two-step reconstruction method for the measured channel base-current waveform of artificially triggered lightning based on the PSO algorithm. This method can obtain the reconstruction parameters of current quickly and accurately.

II. EXPERIMENTS AND THE DATA OF ARTIFICIALLY TRIGGERED LIGHTNING

The Field Experiment Base on Lightning Science of the China Meteorological Administration was jointly established by the Chinese Academy of Meteorological Sciences and the Guangzhou Institute of Tropical and Marine Meteorology, and it is a key field experiment base of the China Meteorological Administration. The experiment base was founded in 2005 and is located in Guangzhou, Guangdong Province. There are more than 80 annual thunderstorm days in this area, which provides good weather conditions for lightning observations and research. The experimental base is composed of three main functional areas. The first functional area is the artificially triggered lightning experiment site, which is 1.9 km away from the Guangliancun (GLC) station of the low-frequency E-field detection array (LFEDA) system [21]–[23]. It is mainly used for triggering artificial lightning and conducting comprehensive observations. Additionally, lightning protection experiments are carried out. The second experimental area is located in the Conghua Meteorological Bureau, and it is mainly used to carry out observations of natural lightning and lightning early warning tasks. The third area is located in the Guangdong Meteorological Bureau, and it is mainly used to carry out the comprehensive observation of optical and electromagnetic fields related to lightning to tall objects in the city [24]–[29]. The actual lightning current data involved in this paper are from the Guangdong Comprehensive Observation Experiment on Lightning Discharge (GCOELD) carried out in 2015.

The triggered lightning experimental field site covers an area of approximately 36,000 m^2, with a main area of approximately 1 km^2. In addition, experimental facilities such as control rooms, generator rooms, automatic weather stations, communication towers, high-voltage transmission lines, and wind turbines have been built. The optical observation point for triggered lightning is approximately 1.9 km from the field experiment site for triggered lightning and is equipped with comprehensive equipment for observing acoustic, optical, electric and magnetic effects related to lightning. The layout of the experiment site is shown in Fig. 1.

Six rocket launchers are installed in the triggered lightning test field. The end of each rocket is connected to a lightning rod with copper wire. The lower part of the lightning rod is connected with a coaxial shunt as a lightning current

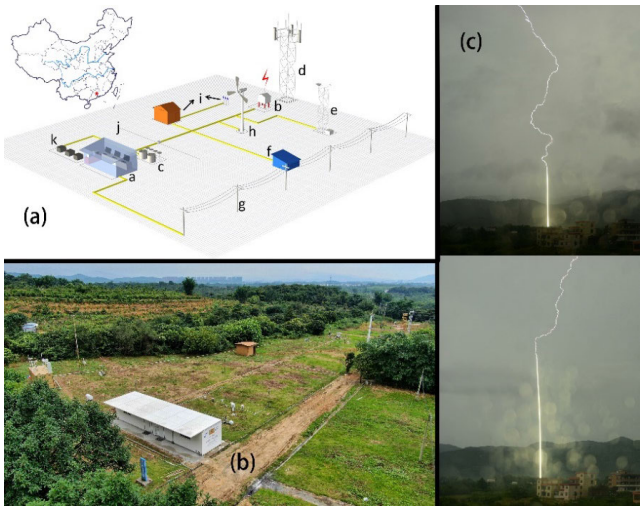

FIGURE 1. Triggered lightning experiment field site. Layout of the test equipment at the triggered lightning field experiment site [27]. a: Control room (rocket launches and data acquisition are conducted from here). b: Wooden house (a lightning rod is installed above it, and current measuring equipment is contained in it). c: Region for measuring electrical parameters. d: Iron tower (a model of a communications tower). e: Automatic weather station. f: Region for testing surge protection devices. g: 10 kV overhead line. h: Wind turbine. i: Petrochemical instrument (sensor and power for the distribution control system). j: Buried cables. k: Shields constructed from brick, concrete, and steel mesh. (b) Aerial photo of the experiment site. (c) Sample photos of artificially triggered lightning.

measuring device, with a resistance of only 1 mΩ and a measuring range of 100 kA. The output voltage of the coaxial shunt passes through the photoelectric converter, and the signal is recorded by a DL750 oscilloscope. The sampling rate is 10 MSa s^{-1}, and the recording length is 2 s. The rocket launch control room is located in a steel room approximately 90 m from the rocket launcher. Special grounding and shielding designs were made for the control room to ensure the safety of personnel and equipment in the room in case of short-distance lightning.

Fig. 2 shows the return-stroke current waveform of an artificially triggered lightning event acquired at 15:25 on August 14, 2015. In nearly 0.8 s, 14 return strokes occurred. The minimum return-stroke peak current was 10.0 kA (R11), and the maximum return-stroke peak current was 30.8 kA (R12). The first return stroke occurred at 25.101 s, with a peak current of 13.3 kA. The local characteristics of the current waveform of R1 are shown in Fig. 2b and c.

The main lightning monitoring instruments set up at the triggered lightning field site are the atmospheric average electric field instrument, the fast antenna (with a decay time constant of 2 ms and a bandwidth of 1 kHz $\sim$ 2 MHz, compare to the fast antenna of the LFEDA system), the slow antenna (with a decay time constant of 6 s and a bandwidth of 10 Hz $\sim$ 3 MHz) and the wide-band magnetic loop antenna (100 Hz $\sim$ 5 MHz). These observations are used to determine whent to launch the rocket and record the electromagnetic signals of lightning triggered in the experiment.

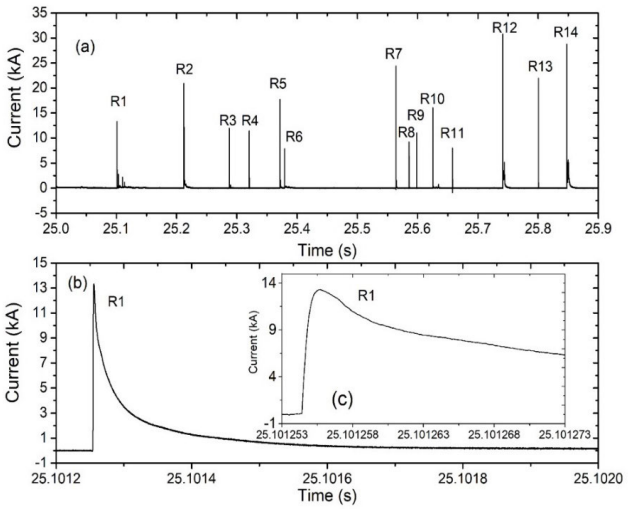

FIGURE 2. At 15:25 on August 14, 2015 (No. 201508141525), the current waveform of a multiple-return-stroke triggered lightning event was obtained, and there were 14 return strokes (a). (b). The long time-sequence (800 μs) current waveform of the first return stroke (R1). (c) The short time-sequence current waveform of R1 (20 μs).

III. PARTICLE SWARM OPTIMIZATION ALGORITHM

In this paper, the parametric reconstruction of the lightning return-stroke current is based on PSO, which is a kind of artificial intelligence algorithm. It is a swarm intelligence algorithm developed by J. Kennedy and R. C. Eberhart [30], [31]. The idea of PSO is derived from research on the predatory behavior of birds and fish, and it simulates the behavior of birds flying and foraging. Birds achieve their goal through collective cooperation, and PSO is an optimization method based on this kind of particle swarm intelligence. It starts from a random solution, finds the optimal solution by iteration, and evaluates the quality of the solution according to fitness. Since it was proposed, PSO has been widely used in many fields, such as computer science, engineering, biology, and economics [26]–[42]. The PSO algorithm has many merits. It is simple to implement, has only a few parameters to be set, it is effective in global search, it is insensitive to scaling of design variables, and it is easily parallelized for concurrent processing [43]–[47].

PSO is a group-based adaptive stochastic optimization algorithm. The PSO algorithm first creates initial particles and assigns them initial velocities. Then, an objective function of each particle position is evaluated, and the best function value and the best position are determined. Next, we choose a new velocity according to the current speed, the best position of the particle and the best position of the group. We iteratively update the particle swarm position (the new position is the old position plus the speed, and the updated particle position remains within the boundary) and speed. The iteration process continues until the algorithm reaches the stop criterion.

In an D-dimensional space (where D is equal to the number of unknown parameters), the position and velocity of particle j are represented by vectors $\mathrm{X}_j = (\mathrm{X}_{j1}, \mathrm{X}_{j2}, \ldots \mathrm{X}_{jD})$ and $V_j = (V_{j1}, V_{j2}, \ldots V_{jD})$, respectively. Let X^k_{pbestj} and X^k_{gbest} be the personal best position of particle j and global best position of group. On the basis of the velocity and distance of X^k_{pbestj} and X^k_{gbest}, the velocity and position of each particle can be modified:

$$V^{k+1}_{jd} = W * V^k_{jd} + C_1 r_1 \left(X^k_{pbestjd} - X^k_{jd}\right) + C_2 r_2 \left(X^k_{gbestd} - X^k_{jd}\right), \quad j = 1, 2, \ldots\ldots N, \; d = 1, 2, \ldots\ldots D, \tag{1}$$

The definition of variables is shown in TABLE 1.

TABLE 1. The variable definition in Section III.

d	dimension index
j	particle index
D	the number of unknown parameters / dimension size
N	The population size of PSO
k	Number of iterations
V^{k+1}_{jd}	Velocity of the d-th variable of the j-th particle in the (k+1)-th iteration
X^k_{jd}	Position of the d-th variable of the j-th particle in the k-th iteration
C_1, C_2	Cognitive and social acceleration factors
$X^k_{pbestjd}$	Personal best value of the d-th variable of the j-th particle in the k-th iteration
X^k_{gbestd}	Global best value of the d-th variable in the k-th iteration
r_1, r_2	Uniformly distributed random numbers generated separately
W	Inertia weight
I^{fit}	Calculated current
I^{obs}	Observed current
g	Grid number of the channel base current participating in the PSO calculation at a 10 MHz sampling rate
L	Data length (for a 10 MHz sampling rate and a 400 μs time length, L = 4000)

The velocity of each particle is updated by formula (1), and the particle position is updated by the following formula:

$$X^{k+1}_{jd} = X^k_{jd} + V^{k+1}_{jd}, \quad j = 1, 2, \ldots\ldots N, \; d = 1, 2, \ldots\ldots D. \tag{2}$$

The process of the PSO algorithm is as Fig. 3:

Generally, the stopping criterion of the algorithm is that the relative change in the fitness function or objective function in the process of iteration is less than a certain threshold value; the maximum number of iterations is reached; or the result of iteration is less than a threshold value near the extreme value of the objective function. In this paper, to obtain the best iterative results, the algorithm stopping criterion is that the relative change of the fitness function is less than a certain threshold value.

The fitness function is an important concept of PSO. The PSO algorithm selects the global optimal solution and the

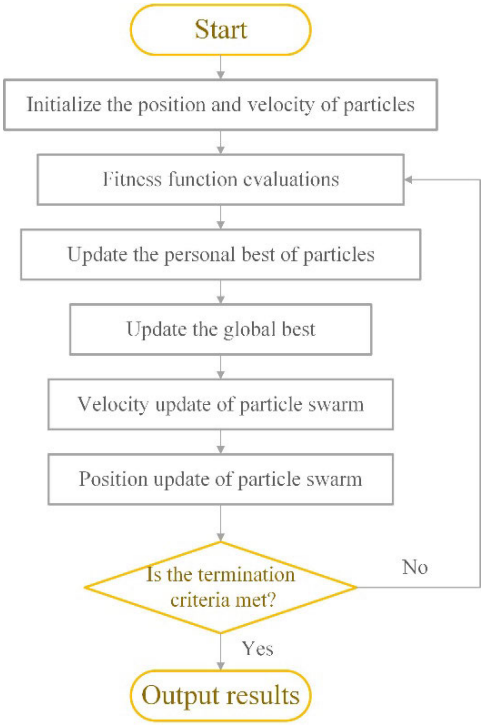

FIGURE 3. Flow chart of the PSO algorithm.

individual optimal solution for a single particle by comparing the fitness value of each particle. The expression of the fitness function is unique to different problems. In this paper, the expression of the fitness function is:

$$Fitness = \frac{1}{L}\sqrt{\sum_{g=1}^{L}\left[I_g^{fit} - I_g^{obs}\right]^2}, \tag{3}$$

IV. RECONSTRUCTION METHOD OF THE RETURN-STROKE CURRENT

A. BASIC CONSTRUCTOR OF THE RETURN-STROKE CURRENT - THE HEIDLER FUNCTION

The international standard IEC 62305-1 ed. 2 (IEC 62305-1, 2010) defines three types of lightning return-stroke current pulses in lightning research and engineering applications. The waveform of these return-stroke currents is defined by the Heidler function [10], [48] with specific parameters, and it is shown in equation (4).

The Heidler function has significant advantages in constructing the return-stroke current waveform compared with some previously used functions, such as the biexponential function [8]. For example, the first derivative of the biexponential function for $t = 0$ is not zero, this is not meaningful in physics, and it means the function is not initially continuous [9]. Unlike the biexponential function, the Heidler function is differentiable and continuous at time $t = 0$, and it has a better ability to construct the return-stroke current waveform. At present, the method of constructing the return-stroke current based on the Heidler function is widely used.

$$I(t) = \frac{I_0}{\eta}\frac{\left(\frac{t}{\tau_1}\right)^n}{\left(\frac{t}{\tau_1}\right)^n + 1}e^{-\frac{t}{\tau_2}}, \tag{4}$$

The definition of variables is shown in TABLE 2

TABLE 2. The variable definition in Section IV.

I_0	Peak current
F	Number of current components
i	Current component index
t	Time
$\tau_1(\tau_{11},\tau_{21},\tau_{31})$	Rise-time constants of the return-stroke current pulse for different current component
$\tau_2(\tau_{12},\tau_{22},\tau_{32})$	Decay-time constants of the return-stroke current pulse for different current component
$n\ (n_1,n_2,n_3)$	Is used to control the order of the current function for different current component
$A\ (A_1,A_1,A_1)$	Corrected peak current for different current component, $A = I_0/\eta$
a	Shape control parameter of current
m	Order of exponential function
η	Current correction coefficient

where η is the current correction coefficient, which is defined as:

$$\eta = exp\left[-\left(\frac{\tau_1}{\tau_2}\right)\left(n\frac{\tau_2}{\tau_1}\right)^{1/n}\right]. \tag{5}$$

The Heidler function contains five unknown parameters (I_0, η, τ_1, τ_2, n), among which the current correction coefficient can be calculated from the other four parameters. Therefore, equation (5) can be simplified and rewritten as follows:

$$I(t) = A \cdot \frac{\left(\frac{t}{\tau_1}\right)^n}{\left(\frac{t}{\tau_1}\right)^n + 1}e^{-\frac{t}{\tau_2}}, \tag{6}$$

where $A = I_0/\eta$, which is called the corrected peak current in this paper. The return-stroke current function is now composed of four unknown parameters (A, τ_1, τ_2, n). A return-stroke current waveform constructed by the Heidler function is shown in Fig. 4a. The parameters are specified by IEC 62305-1 ed. 2 (IEC 62305-1, 2010) for the subsequent negative impulse.

Some studies have also shown that, on the basis of the Heidler function, the sum of two Heidler functions (Fig. 4b) [11], [12] or the sum of a Heidler function and other functions (Fig. 4c and d) [13] can construct the return stroke current better to a certain extent, and the current components constructed by each Heidler function (or other functions) have different physical meanings. These models

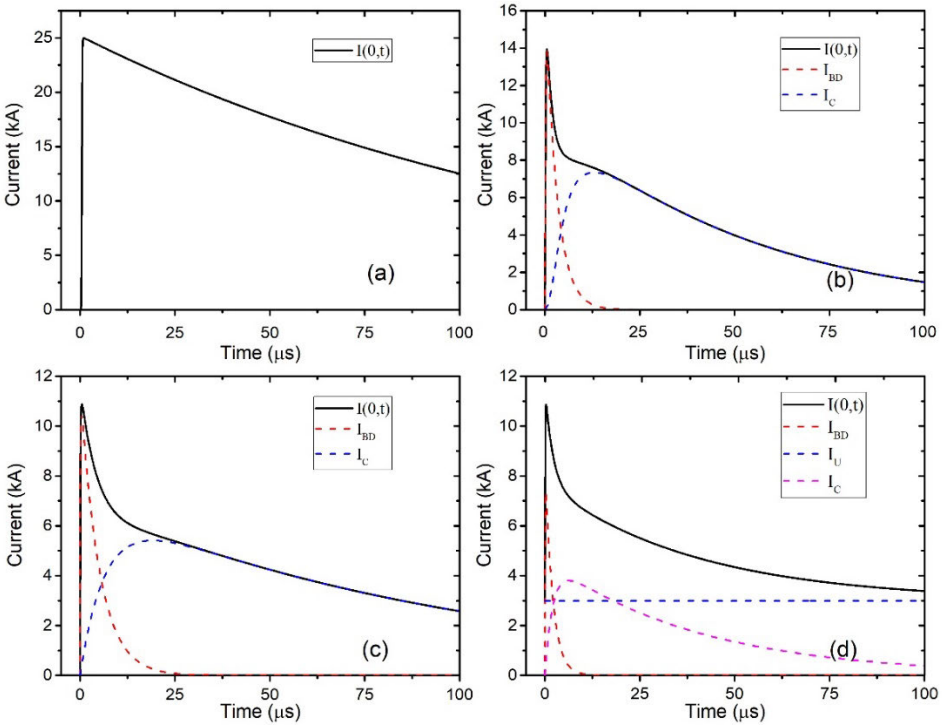

FIGURE 4. The return-stroke current constructed by different current construction methods. (a) One Heidler function; (b) sum of two Heidler functions; (c) sum of one Heidler function and one biexponential function; (d) sum of one Heidler function, one biexponential function and one uniform current. (Note: for convenience of comparison, the current simulation time length is uniformly 100 μs),

play an important role in understanding the physical process of lightning discharge and its engineering and scientific research applications under the condition of the relatively limited electronic computing capacity available at the end of the last century.

However, there are some shortcomings in these current construction models. First, a single Heidler function cannot perfectly construct a current waveform that is exactly consistent with the measured return-stroke current. The current construction model, which sums two Heidler functions or a Heidler function and an exponential function, can reconstruct the current waveform more accurately only on the time scale of a few microseconds to tens of microseconds; on a longer time scale (hundreds of microseconds), the error in constructing the current waveform increases significantly (as shown in Fig. 5). The error is usually larger in constructing a strong return stroke current with a peak current of tens of kA. In addition, as is done in some construction models, a uniform current is added to the current (Fig. 4d). Although this has a physical meaning, it conflicts with the observed facts, as it prevents the current from decaying to 0.

Taking the current construction model of the sum of two Heidler functions as an example, we examine R7 in Fig. 2 (the peak current is 24.4 kA) and use the PSO algorithm to determine the construction parameters of a group of two Heidler functions to minimize the fitness in formula (3). As shown in Fig. 5a, the current construction parameters obtained with a 40 μs current waveform can make the measured current and the simulated current coincide well on a short time scale of 20 μs. After 20 μs, the difference between the measured current and the simulated current increases gradually; when using this set of parameters to calculate the current waveform on a longer time scale, the error increases significantly (as shown in Fig. 5b). For such a strong return-stroke current, as shown in Fig. 5, the transferred charge ratio after 20 μs is close to approximately 50% of the total charge transferred by the return stroke. Therefore, there is a large error in the current reconstruction in the short time series, which limits the application scenarios of the constructed current and the construction parameters.

B. CONSTRUCTOR OF A LONG TIME-SERIES TRIGGERED LIGHTNING RETURN-STROKE CURRENT

From the research practice, we found that in a short time series of 20 μs, the sum of two Heidler functions (formula 7) can be used to construct the return stroke current, and a group of parameters can be found by the PSO algorithm that can reconstruct the current waveform accurately to a certain extent [20], [40]. However, as described in Section 4.1, the construction method of the sum of the two groups of functions is not suitable for the waveform reconstruction of a lightning return-stroke current with a long time series.

$$I(t) = A_1 \cdot \frac{\left(\frac{t}{\tau_{11}}\right)^{n_1}}{\left(\frac{t}{\tau_{11}}\right)^{n_1}+1} e^{-\frac{t}{\tau_{12}}} + A_2 \cdot \frac{\left(\frac{t}{\tau_{21}}\right)^{n_2}}{\left(\frac{t}{\tau_{21}}\right)^{n_2}+1} e^{-\frac{t}{\tau_{22}}} \quad (7)$$

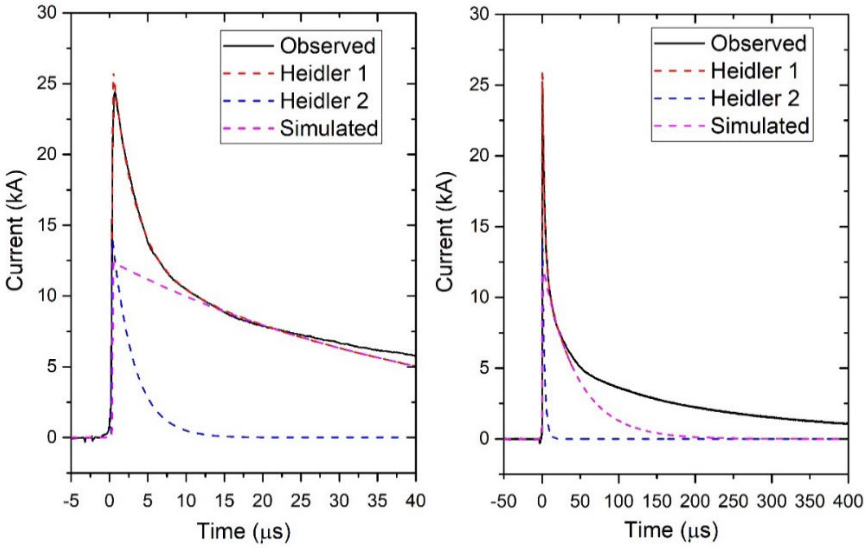

FIGURE 5. Taking R7 in Fig. 2 as an example, the current construction parameters of two Heidler functions are obtained by using the PSO algorithm for 40 μs of measured current, and a comparison between the reconstructed current and the measured current on different time scales is made. (a) A short time series of 40 μs; (b) a long time series of 400 μs.

The lightning research team of the Chinese Academy of Meteorological Sciences has been engaged in observations and research on triggered lightning. A fixed-field comprehensive lightning observation base has been established in the Conghua district, Guangzhou, China (GCOELD). For more than ten years, observations and experiments with natural and triggered lightning have been carried out during the summer. By 2020, the research team had successfully triggered more than 200 artificially triggered lightning events and accumulated channel base current data for thousands of triggered lightning return strokes. Based on the Heidler function, the following functions are proposed as constructors of the triggered lightning return stroke current by studying the characteristics of the long time-series waveforms of a large number of measured current data:

$$I(t) = \begin{cases} \sum_{i=1}^{F} A_i \cdot \dfrac{\left(\frac{t}{\tau_{i1}}\right)^{n_i}}{\left(\frac{t}{\tau_{i1}}\right)^{n_i}+1} e^{-\frac{t}{\tau_{i2}}}, & F=2 \text{ or } F=3 \quad (8) \\ \sum_{i=1}^{F} A_i \cdot \dfrac{\left(\frac{t}{\tau_{i1}}\right)^{n_i}}{\left(\frac{t}{\tau_{i1}}\right)^{n_i}+1} e^{-\frac{t}{\tau_{i2}}} + A_3 \\ \cdot \dfrac{\left(\frac{t}{\tau_{31}}\right)^{n_3}}{\left(\frac{t}{\tau_{31}}\right)^{n_3}+1} e^{-\left(a\cdot\frac{t-\tau_{31}}{k}\right)^{m}}, & F=1 \text{ or } F=2 \quad (9) \end{cases}$$

where, in formula (9), $k = (\tau_{32} - \tau_{31})/\tau_{31}$.

From the definitions of (8) and (9), we can see that based on the Heidler function, according to the waveform characteristics of the return-stroke current, triggered lightning return-stroke currents can be divided into two types. As shown in Fig. 6, the difference between the two current waveforms

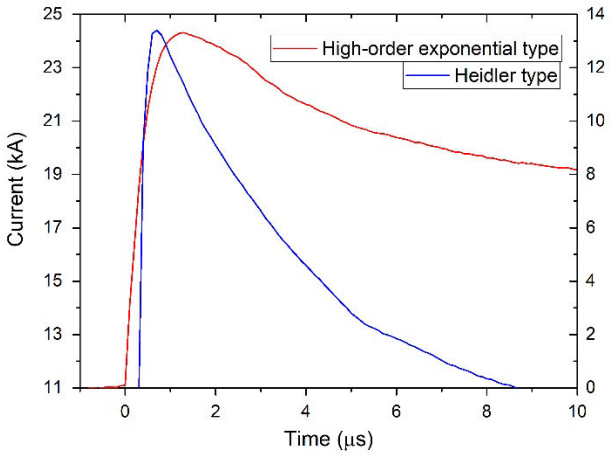

FIGURE 6. Comparison of the return-stroke current waveforms of two different head features (the left coordinate is the current value of the blue curve, and the right coordinate is the current value of the red curve).

shows that they have different peak waveform characteristics. As shown by the blue line in Fig. 6, the head of the current waveform has a "shrinking" form, with fast rising and falling edges; i.e., the current has a high rate of change. This waveform feature can be constructed by the classical Heidler function. Therefore, we say that a current with this morphological feature is of the Heidler type. The other type is shown by the red line in Fig. 6. The head feature of the current takes an "outward expansion" form, with relatively slow rising and falling edges. The rate of change of the current is relatively slow compared with that of the Heidler type. The exponential part of the Heidler function is not sufficient to construct the falling edge of this type of current. Therefore, for the second type, we transform the Heidler function into

TABLE 3. The Current Reconstruction Parameters of R1, R11 and R13 Shown in this Paper.

Parameter / Number	I_C				I_{QU}				I_{BD}					
	τ_{11} μs	τ_{12} μs	A_1 kA	n_1	τ_{21} μs	τ_{22} μs	A_2 kA	n_2	τ_{31} μs	τ_{32} μs	A_3 kA	n_3	a	m
R1	0.13	21.95	7.87	1.49	0.31	152.31	3.40	6.76	0.67	78.76	2.88	38.56	5.36	2.14
R11	0.20	13.10	3.47	16.60	0.0001	124.12	2.46	1.00	0.40	1.69	4.13	2.57		
R13	0.024	37.01	10.90	1.00	0.195	126.16	6.80	79.44	0.35	3.58	6.81	2.46		

the form of $A_3 \cdot \frac{\left(\frac{t}{\tau_{31}}\right)^{n_3}}{\left(\frac{t}{\tau_{31}}\right)^{n_3}+1} e^{-\left(a \cdot \frac{t-\tau_{31}}{k}\right)^m}$ in formula (9), referring to the construction method of the exponential function used in some studies [49]–[56]. According to the inversion calculation of the measured current waveform by PSO, it is found that for this type of current waveform, the value of m is greater than 1, so we call this type of current waveform a high-order exponential type (for example, as shown in TABLE 3, $m = 2.14$ for R1).

The value of F in formulas (8) and (9) varies, because for a weak current (a peak current of several kA) or a return stroke process with a weak continuous current, the sum of two functions is usually sufficient for the construction of the full current waveform.

Regarding the components of the long-time series return-stroke current, we noted that as early as the 1990s, some scholars proposed a similar current construction model and applied the constructed current to the study of the return stroke model [14]. It is believed that the return-stroke current of the ground flash consists of three components—namely, the breakdown current, corona current and uniform current (as shown in Fig. 4d)—which fits with the idea of return-stroke current reconstruction adopted in this paper. However, as seen in the analysis above, a uniform current does not exist in the actual measured return-stroke current. In early research, an approximation of the uniform current was used to represent the quasi-uniform part of the current waveform with the longest duration and the slowest change. As shown in Fig. 5, the summation of the two functions cannot construct the feature of slow change in the long time-series return-stroke current. However, at the end of the last century, the approximation of the uniform current under the condition of limited electronic computing capacity was of great physical and practical significance.

C. TWO-STEP PARAMETERIZED RECONSTRUCTION METHOD

Our study shows that a Heidler function can be used to construct the quasi-uniform part of the long time-series return-stroke current exactly. Similar to the proposal of Lin *et al.* [14], another Heidler function can be used to construct a current component similar to the corona current. Lin *et al.* [14] considered the waveform of the head of the return stroke current to be generated by the breakdown process, and it is called the breakdown pulse current. This is similar to our strategy of using a Heidler function or a high-order exponential function to construct the local waveform of the head of the return-stroke current waveform. Therefore, in this paper, we follow their representation of current component characteristics and call the three components in the long time-series return-stroke current waveform constructor the breakdown current, corona current and quasi-uniform current, as shown in Fig. 7. This is the basic model used to calculate the current components and achieve the parametric reconstruction of the measured current with the PSO algorithm.

Yang *et al.* [20] applied the PSO algorithm to the calculation of the measured current reconstruction parameters of triggered lightning and reconstructed the channel base current waveform of a 40 μs, relatively short time-series with the parametric model of the sum of two Heidler functions. As shown in Fig. 5, employing the sum of two Heidler functions to reconstruct the return-stroke current waveform is only effective on a time scale of tens of microseconds. Although the reconstructed current is somewhat accurate, the reconstructed current waveform is completely distorted when the construction parameters obtained are used to calculate the current waveform of a longer time series. The work of Yang *et al.* [20] shows objectively that the PSO algorithm can play a role in the parametric reconstruction of multiparameter current waveforms (8 unknown parameters, with components $[\tau_{11}, \tau_{12}, A_1, n_1, \tau_{21}, \tau_{22}, A_2, n_2]$).

However, we find that although the PSO algorithm can obtain the solutions of 8 unknown parameters, it cannot find 12 (formula (8)) or 14 (formula (9)) position parameters when the swarm is 100 times larger, so formula (3) is the minimum case. We think that this is because when three groups of parameters are identical or approximately the same, the PSO algorithm easily falls into a local minimum solution and cannot find the global optimal solution.

Therefore, on the basis of three current component models, to accurately obtain the parameters of a lightning return-stroke current using the PSO algorithm and to perform the parametric reconstruction of a long time-series channel base current, this paper proposes a two-step reconstruction

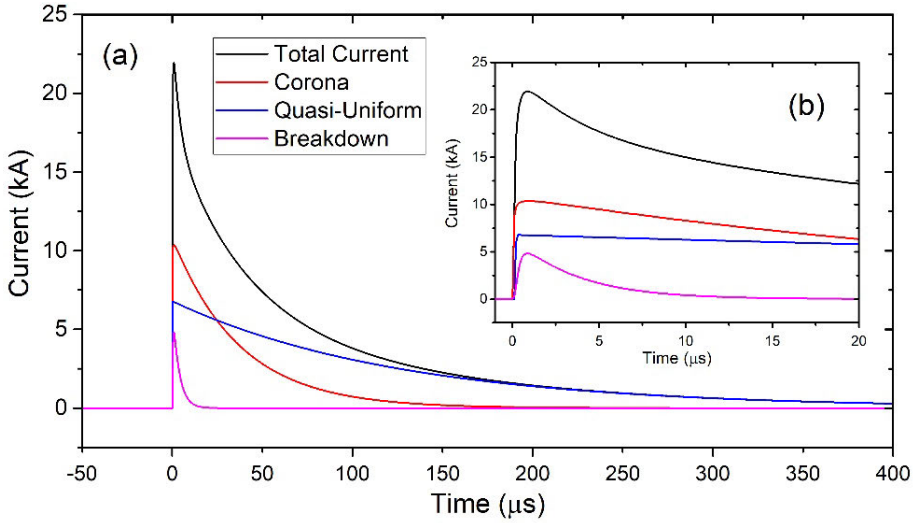

FIGURE 7. The three components of the triggered lightning return-stroke current (the current parameters in the diagram are from the PSO calculation results for R13 in Fig. 2, the value of parameters calculated by PSO are shown in TABLE 3).

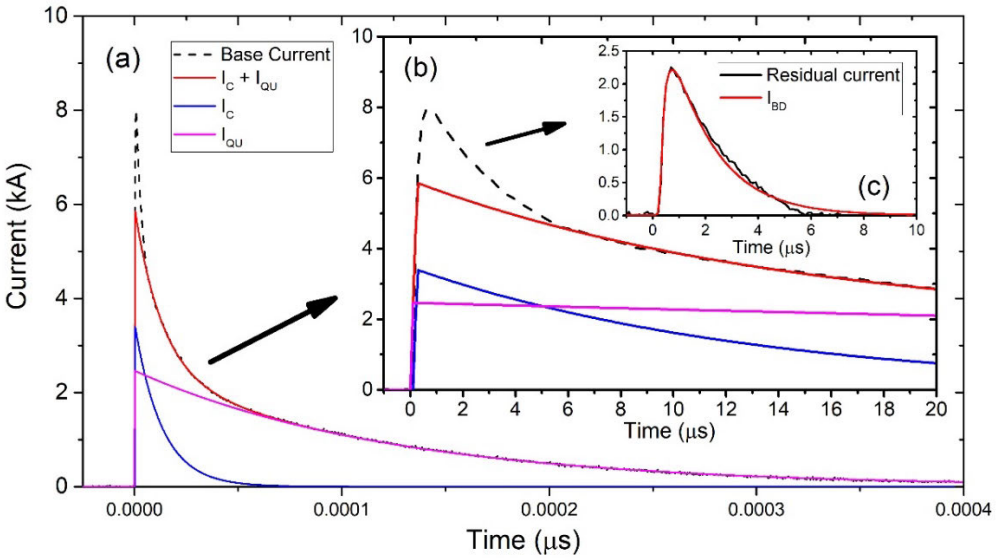

FIGURE 8. Schematic diagram of the two-step current reconstruction method. (a) Find $I_C + I_{QU}$; (b) calculate the residual current, i.e., the base current minus $I_C + I_{QU}$; (c) calculate I_{BD} according to the residual current. (The current parameters in the schematic are from R11 in Fig. 2 and its PSO calculation results, the value of parameters calculated by PSO are shown in TABLE 3).

method for the lightning return-stroke current waveform based on the PSO algorithm. As shown in Fig. 8, the main flow of the two-step reconstruction method is to find the construction parameters of I_C and I_{QU} with the PSO algorithm based on the morphological characteristics of the return-stroke current waveform so that $I_C + I_{QU}$ is consistent with the base current to the greatest extent. In this way, the difference between the base current and $I_C + I_{QU}$ is only the part shown by the dotted line in Fig. 8a and b, that is, around the time of the peak of the return-stroke current waveform, which is usually less than 10 μs in width. We calculate the residual current and set the residual current equal to the difference between the base current and $(I_C + I_{QU})$; then, we judge whether the current is a Heidler type or high-order exponential type according to the waveform characteristics of the residual current to select the appropriate constructor. Then, we use the PSO algorithm to find the breakdown current component (as shown in Fig. 8c).

V. CURRENT RECONSTRUCTION AND EVALUATION OF MULTIPLE-STROKE TRIGGERED LIGHTNING

By using the two-step method proposed in this paper, we carry out the parametric reconstruction of the measured return-stroke current waveform of triggered lightning.

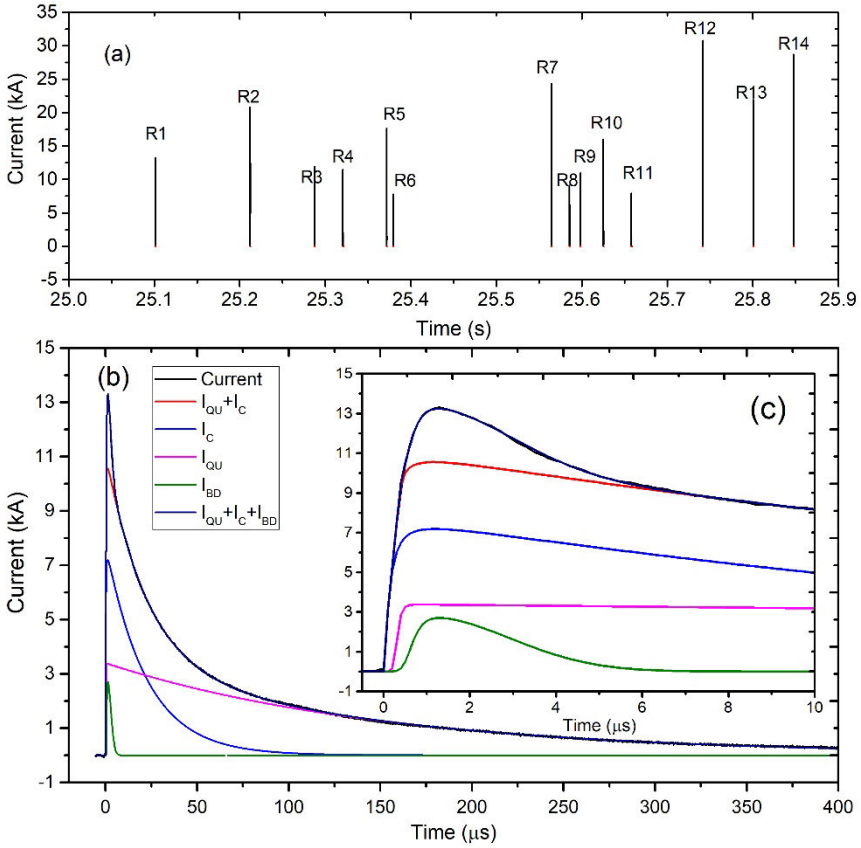

FIGURE 9. (a) The reconstructed waveform of the multistroke artificially triggered lightning (No. 201508141525); (b) The comparison between the reconstructed current of R1 and the measured current, where the current components are shown in the figure; (c) The reconstructed current of R1 is amplified locally for 10 μs, and the shape of its I_{BD} is a high-order exponential type (formula (9)). (The value of parameters calculated by PSO are shown in TABLE 3).

According to the current examples, based on the parametric model and reconstruction method, the parametric reconstruction of the channel base current waveform can be achieved almost perfectly. Here, we take the example of multi-return-stroke triggered lightning as shown in Fig. 2 and illustrate the accuracy of the parametric model and the effectiveness of the reconstruction method on the basis of four characteristics: the waveform error of the measured current and the reconstructed current (evaluated by formula 3), the error of the current change rate (dI/dt, evaluated by formula 3), the peak current error and the error of the transferred charge (time integration of the current).

As shown in Fig. 9a, a complete reconstruction of the triggered lightning current with 14 return strokes shown in Fig. 2 is achieved by the two-step reconstruction method proposed in this paper. R2 is reconstructed by a 20 μs short time-series current, and the other 13 return strokes are reconstructed by a 400 μs long time-series current. This is because R2 has a large M component after the peak time of 22 μs, which means the current waveform of the long time series does not conform to the reconstruction model of formula (8) or (9). In addition, in the current waveform of the 14 return strokes, except for R1 and R2, the shape of I_{BD} is of the Heidler type.

To facilitate research and application, TABLE 3 lists the parameters of the reconstructed current of the three return-stroke examples shown in this paper.

After constructing the parametric model, proposing the two-step reconstruction method for triggered lightning return-stroke current, and achieving the parametric reconstruction of triggered lightning current cases, we evaluate the accuracy of the model and the effectiveness of the reconstruction method from the perspectives below. It should be noted that R2 is reconstructed from a short time series, and the number of data points is far less than that obtained for 400 μs at 20 μs and 10 M sampling rates. For the error evaluation method defined by formula (3), the data length is too different from that in the other cases to be comparable to them. Therefore, R2 is not considered in the following evaluation and comparison, and only the 13 other return strokes are considered.

(a) Error of the current I and current change rate dI/dt:

The core idea of the PSO algorithm is to determine a set of parameters so that the measured signal and the simulated

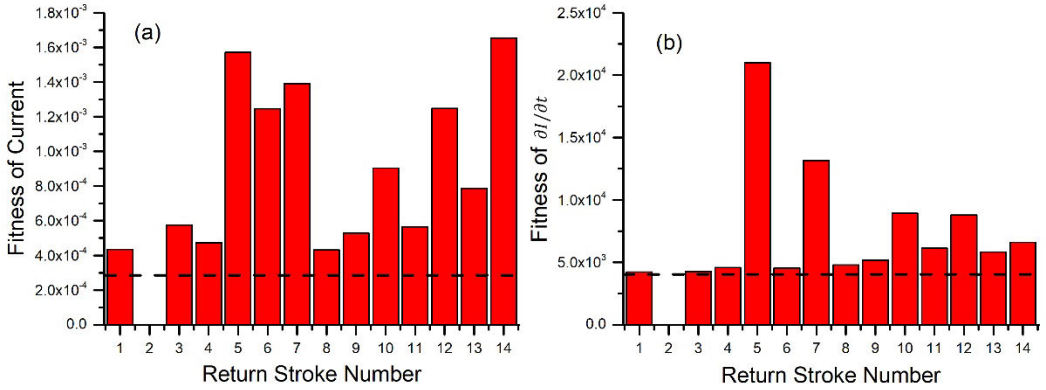

FIGURE 10. The error between the measured current and reconstructed current and the error in the current change rate. The dotted lines in the figures represent the error between the measured white noise and the 0-axis (a) and the error between the change rate of the measured white noise and the 0-axis (b).

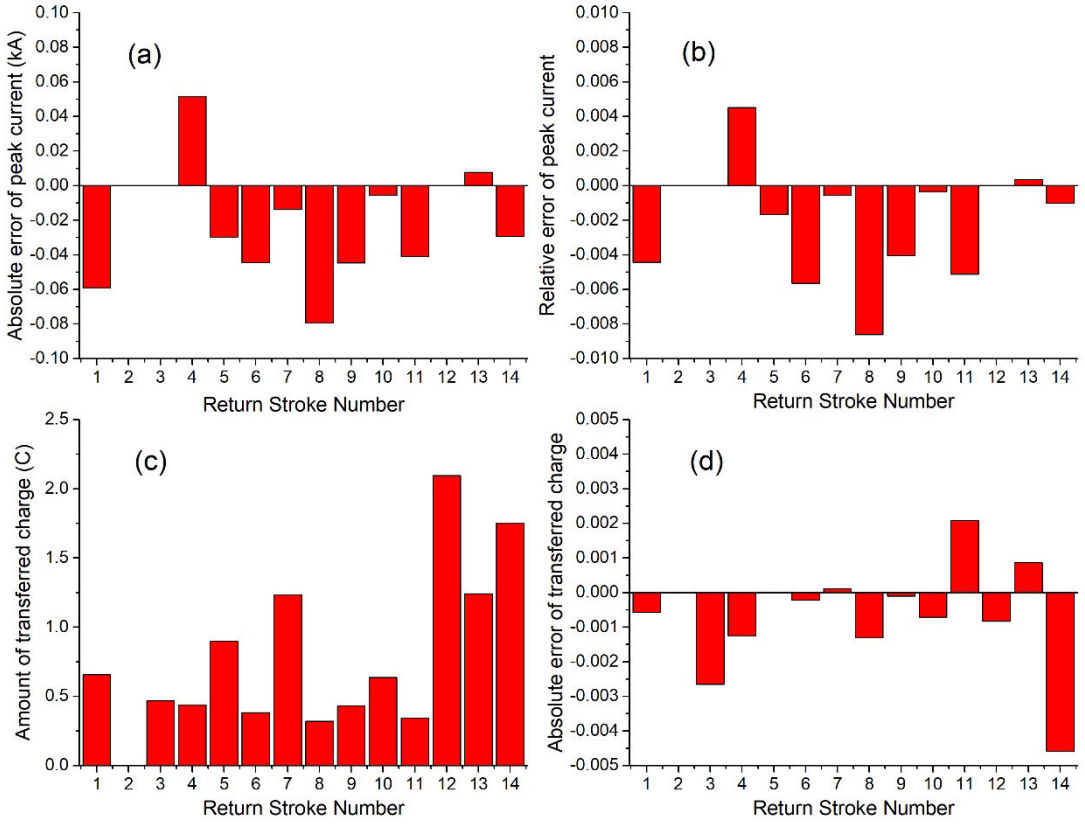

FIGURE 11. Error in the peak value of the reconstructed current and the statistics of the transferred charge and error. (a) Absolute error of the peak value of the reconstructed current; (b) Relative error of the peak value of the reconstructed current; (c) Statistics of the transferred charge of the reconstructed current in a long time series of 400 μs; (d) Absolute error of the transferred charge of the reconstructed current in a long time series of 400 μs.

signal are as similar as possible (the error is the smallest), where the error of the two signals is defined by formula (3). Therefore, the error between the measured current and the reconstructed current of 400 μs is calculated by formula (3). In addition, considering that in many engineering applications, the change rate (dI/dt) of the return-stroke current is an important parameter for calculating the various effects of the return stroke, the error between the measured current (dI/dt) and the reconstructed current (dI'/dt) is also calculated by formula (3). Since the fast range of the return-stroke current is usually only the first few microseconds, the time range for calculating the error of dI/dt is only the first 20 μs of the current.

In Fig. 10, the error of the measured current and the reconstructed current (Fig. 10a) and the error of dI/dt (Fig. 10b) are shown. The dotted lines in the figures represent the error

of the measured white noise signal and axis 0 and the error of the measured white noise change rate and axis 0. Generally, the error between the reconstructed current waveform and the measured current waveform of the 13 return strokes is small in the long time series of 400 μs, and the reconstructed current and measured current may almost be the same. Especially for the dI/dt of the first 20 μs of current, the dI'/dt of the reconstructed current is more consistent with the dI/dt of the measured current, and the error between the two is almost equal to the error between the change rate of the white noise and the 0-axis. In Fig. 10, the cases with slightly larger errors are all due to the weak disturbance current in the measured current in the observed time window.

(b) Error in the peak current and error in the transferred charge quantity:

Fig. 11a and b show the absolute and relative errors, respectively, between the peak value of the reconstructed current and the measured current. Compared with the peak value of the measured current, the absolute error of the peak value of the reconstructed current is generally small, only tens of amperes, which is equivalent to the amplitude of the Gaussian white noise in the measured current. Accordingly, the relative error of the peak current is less than 1%. All of these results show the accuracy of the improved parametric scheme for triggered lightning return-stroke current and the excellent performance of the two-step reconstruction method based on the PSO algorithm.

Fig. 11c shows the time integration of the 13 measured currents, i.e., the amount of charge transferred by the return stroke:

$$Q = \int_0^t I(\tau)\, d\tau, \quad t = 400\mu s \tag{10}$$

It can be seen from the figure that the amount of transferred charge of these 13 return strokes varies from 0.32 C (R8) to 2.1 C (R12), with a wide range of variation. Fig. 11d shows that the error of the transferred charge calculated by the reconstructed current can be ignored. The maximum error of R14 is 0.0046 C, which is much larger than that of the other return strokes. This is because there is a certain amplitude of the disturbance current at the end of the R14 current, which leads to a local deviation between the reconstructed current and the measured current.

VI. CONCLUSION

It is of great significance to study the measured return-stroke current of artificially triggered lightning and to reconstruct it parametrically. This is helpful not only in understanding the characteristics of the physical process of lightning but also in developing related models; it is also of great reference value for various engineering applications. In this paper, the improvement of the constructor of the return-stroke current waveform in a long time series and its parametric reconstruction method are explored.

On the basis of the waveform characteristics of the measured channel base current data of artificially triggered lightning obtained by the lightning research team of the Chinese Academy of Meteorological Sciences over a long period of time, combined with an early theoretical model of the return-stroke current, this paper divides the long time-series return-stroke current into three components: the breakdown current, corona current and quasi-uniform current. According to the construction characteristics of the three components, and based on the Heidler function, a three-component constructor of the return-stroke current is proposed: the corona current and quasi-uniform current are constructed by Heidler functions. Depending on the waveform characteristics of the current peak, the breakdown current is constructed by a Heidler function (Heidler type) or a modified exponential function (high-order exponential type) in this paper.

According to the above three-component model of the return-stroke current, this paper proposes a two-step parametric reconstruction method based on the PSO algorithm for the long time-series return stroke current of triggered lightning. The main process of the two-step reconstruction method is to find the construction parameters of I_C and I_{QU} with the PSO algorithm based on the morphological characteristics of the current waveform so that $I_C + I_{QU}$ is as consistent with the channel base current as possible. The difference between the measured current and $I_C + I_{QU}$ is used to calculate the residual current. Then, according to the waveform characteristics of the residual current, we can judge whether it is a Heidler type or a high-order exponential type in order to select the appropriate constructor; then, we use the PSO algorithm to obtain the breakdown current (I_{BD}) component.

In this paper, the parametric reconstruction results of artificially triggered lightning with 14 return strokes are also given, and the accuracy of the reconstructed current of 13 return strokes in a long time series (400 μs) is compared with the measured current from multiple perspectives. The results show that the reconstructed current has a high accuracy in terms of the error between the reconstructed current waveform and the measured current waveform, the error between the change rate of the reconstructed current and the measured current (current differential dI/dt), the error of the current peak value and the amount of charge transferred by the current (time integration of the current), etc. Thus, it is shown that the parametric construction model of the long time-series return-stroke current of triggered lightning given in this paper is accurate, and the two-step current reconstruction method based on the PSO algorithm proposed in this paper is reliable.

ACKNOWLEDGMENT

The authors would like to thank the Editors and the anonymous reviewers for their constructive comments and suggestions, which greatly helped them to improve the technical quality and presentation of this paper.

REFERENCES

[1] V. A. Rakov and M. A. Uman, *Lightning Physics and Effects*. Cambridge, U.K.: Cambridge Univ. Press, 2003.

[2] Y. B. Zeldovich and Y. P. Raizer, *Physics of Shock Waves and High-Temperature Hydrodynamic Phenomena*. New York, NY, USA: Dover, 1965.

[3] W. J. Borucki and W. L. Chameides, "Lightning: Estimates of the rates of energy dissipation and nitrogen fixation," *Rev. Geophys.*, vol. 22, no. 4, pp. 363–372, Nov. 1984, doi: 10.1029/RG022i004p00363.

[4] Y. Wang, A. W. DeSilva, G. C. Goldenbaum, and R. R. Dickerson, "Nitric oxide production by simulated lightning: Dependence on current, energy, and pressure," *J. Geophys. Res., Atmos.*, vol. 103, no. D15, pp. 19149–19159, Aug. 1998, doi: 10.1029/98JD01356.

[5] V. Cooray and M. Rahman, "Efficiencies for production of NOx and o3 by streamer discharges in air at atmospheric pressure," *J. Electrostatics*, vol. 63, nos. 6–10, pp. 977–983, Jun. 2005, doi: 10.1016/j.elstat.2005.03.071.

[6] R. Zhang, G. Zhang, Y. Li, Y. Wang, B. Wu, H. Yu, and Y. Liu, "Estimate of NOX production in the lightning channel based on three-dimensional lightning locating system," *Sci. China Earth Sci.*, vol. 57, no. 7, pp. 1613–1625, Jul. 2014, doi: 10.1007/s11430-013-4812-1.

[7] F. Heidler, J. M. Cvetic, and B. V. Stanic, "Calculation of lightning current parameters," *IEEE Trans. Power Del.*, vol. 14, no. 2, pp. 399–404, Apr. 1999, doi: 10.1109/61.754080.

[8] C. E. R. Bruce and R. H. Golde, "The lightning discharge," *Inst. Elect. Eng.*, vol. 88, no. 6, pp. 487–505, Dec. 1941.

[9] R. B. Anderson and A. J. Eriksson, "Lightning parameters for engineering application," *Electra*, vol. 69, pp. 65–102, 1980.

[10] F. Heidler, "Travelling current source model for LEMP calculation," in *Proc. 6th Intl. Symp. Electromag. Compat.*, Zurich, Switzerland, 1985, pp. 157–162.

[11] C. A. Nucci and F. Rachidi, "Experimental validation of a modication to the transmission line model for LEMP calculation," in *Proc. 8th Symp. Tech. Exhib. Electromagn. Compat.*, Zurich, Switzerland, Mar. 1989, pp. 389–394.

[12] G. Diendorfer and M. A. Uman, "An improved return stroke model with specified channel-base current," *J. Geophys. Res. Atmos.*, vol. 95, no. D9, pp. 13621–13644, Aug. 1990, doi: 10.1029/JD095iD09p13621.

[13] C. A. Nucci, G. Diendorfer, M. A. Uman, F. Rachidi, M. Ianoz, and C. Mazzetti, "Lightning return stroke current models with specified channel-base current: A review and comparison," *J. Geophys. Res. Atmos.*, vol. 95, no. D12, pp. 20395–20408, Nov. 1990, doi: 10.1029/JD095iD12p20395.

[14] Y. T. Lin, M. A. Uman, and R. B. Standler, "Lightning return stroke models," *J. Geophys. Res. Oceans*, vol. 85, no. C3, pp. 1571–1583, Mar. 1980, doi: 10.1029/JC085iC03p01571.

[15] S. Vujević, D. Lovrić, and I. Jurić-Grgić, "Least squares estimation of Heidler function parameters," *Eur. Trans. Elect. Power*, vol. 21, pp. 329–344, 2011.

[16] K. Lundengård, M. Rančić, V. Javor, and S. Silvestrov, "Estimation of pulse function parameters for approximating measured lightning currents using the Marquardt least-squares method," in *Proc. Int. Symp. Electromagn. Compat.*, Sep. 2014, pp. 571–576.

[17] K. Lundengård, M. Rančić, V. Javor, and S. Silvestrov, "Application of the multi-peaked analytically extended function to representation of some measured lightning currents," *Serbian J. Electr. Eng.*, vol. 13, no. 2, pp. 1–11, 2016.

[18] K. Chandrasekaran and G. S. Punekar, "Use of genetic algorithm to determine lightning channel-base current-function parameters," *IEEE Trans. Electromagn. Compat.*, vol. 56, no. 1, pp. 235–238, Feb. 2014.

[19] P. Liu, G. N. Wu, B. Sui, R. F. Li, X. B. Cao, C. L. Fan, and W. Jiang, "Simulation research on the lightning current waveform parameter estimation," *Proc. Chin. Soc. Electr. Eng.*, vol. 29, no. 34, pp. 115–121, 2009.

[20] G. Yang, F. Zhou, Y. Ma, Z. Yu, Y. Zhang, and J. He, "Identifying lightning channel-base current function parameters by powell particle swarm optimization method," *IEEE Trans. Electromagn. Compat.*, vol. 60, no. 1, pp. 182–187, Feb. 2018, doi: 10.1109/TEMC.2017.2705485.

[21] X. P. Fan, Y. J. Zhang, D. Zheng, Y. Zhang, W. T. Lyu, H. Y. Liu, and L. T. Xu, "A new method of three-dimensional location for low-frequency electric field detection array," *J. Geophys. Res., Atmos.*, vol. 123, no. 16, pp. 8792–8812, Aug. 2018, doi: 10.1029/2017JD028249.

[22] X. Fan, Y. Zhang, Q. Yin, Y. Zhang, and D. Zheng, "Characteristics of a multi-stroke 'bolt from the blue' lightning-type that caused a fatal disaster," *Geomatics, Natural Hazards Risk*, vol. 10, no. 1, pp. 1425–1442, Jun. 2019, doi: 10.1080/19475705.2018.1553800.

[23] X. Fan, Y. Zhang, P. R. Krehbiel, Y. Zhang, D. Zheng, W. Yao, L. Xu, H. Liu, and W. Lyu, "Application of ensemble empirical mode decomposition in low-frequency lightning electric field signal analysis and lightning location," *IEEE Trans. Geosci. Remote Sens.*, pp. 1–15, 2020, doi: 10.1109/TGRS.2020.2991724.

[24] W. Lu, L. Chen, Y. Zhang, Y. Ma, Y. Gao, Q. Yin, S. Chen, Z. Huang, and Y. Zhang, "Characteristics of unconnected upward leaders initiated from tall structures observed in Guangzhou," *J. Geophys. Res. Atmos.*, vol. 117, Oct. 2012, Art. no. 019211, doi: 10.1029/2012JD018035.

[25] W. Lu, L. Chen, Y. Ma, V. A. Rakov, Y. Gao, Y. Zhang, Q. Yin, and Y. Zhang, "Lightning attachment process involving connection of the downward negative leader to the lateral surface of the upward connecting leader," *Geophys. Res. Lett.*, vol. 40, no. 20, pp. 5531–5535, Oct. 2013, doi: 10.1002/2013GL058060.

[26] D. Zheng, Y. Zhang, W. Lu, Y. Zhang, W. Dong, S. Chen, and J. Dan, "Optical and electrical observations of an abnormal triggered lightning event with two upward propagations," *Acta Meteorologica Sinica*, vol. 26, no. 4, pp. 529–540, Aug. 2012, doi: 10.1007/s13351-012-0411-x.

[27] D. Zheng, Y. Zhang, Y. Zhang, W. Lu, X. Yan, S. Chen, L. Xu, Z. Huang, J. You, R. Zhang, and Z. Su, "Characteristics of the initial stage and return stroke currents of rocket-triggered lightning flashes in southern China," *J. Geophys. Res., Atmos.*, vol. 122, no. 12, pp. 6431–6452, Jun. 2017, doi: 10.1002/2016JD026235.

[28] Y. Zhang, S. Yang, W. Lu, D. Zheng, W. Dong, B. Li, S. Chen, Y. Zhang, and L. Chen, "Experiments of artificially triggered lightning and its application in conghua, guangdong, China," *Atmos. Res.*, vols. 135–136, pp. 330–343, Jan. 2014, doi: 10.1016/j.atmosres.2013.02.010.

[29] Y. Zhang, W. Lü, S. Chen, D. Zheng, Y. Zhang, X. Yan, L. Chen, W. Dong, J. Dan, and H. Pan, "A review of advances in lightning observations during the past decade in Guangdong, China," *J. Meteorolog. Res.*, vol. 30, no. 5, pp. 800–819, Aug. 2016, doi: 10.1007/s13351-016-6928-7.

[30] J. Kennedy and R. Eberhart, "Particle swarm optimization," in *Proc. ICNN Int. Conf. Neural Netw.*, Perth, WA, Australia, Nov. 1995, pp. 1942–1948.

[31] Eberhart and Y. Shi, "Particle swarm optimization: Developments, applications and resources," in *Proc. Congr. Evol. Comput.*, May 2001, pp. 81–86.

[32] M. A. Abido, "Optimal power flow using particle swarm optimization," *Int. J. Elect. Power Energy Syst.*, vol. 24, no. 7, pp. 563–571, 2002, doi: 10.1016/S0142-0615(01)00067-9.

[33] Z.-L. Gaing, "A particle swarm optimization approach for optimum design of PID controller in AVR system," *IEEE Trans. Energy Convers.*, vol. 19, no. 2, pp. 384–391, Jun. 2004, doi: 10.1109/TEC.2003.821821.

[34] R. Shaw and S. Srivastava, "Particle swarm optimization: A new tool to invert geophysical data," *Geophysics*, vol. 72, no. 2, pp. F75–F83, Mar. 2007, doi: 10.1190/1.2432481.

[35] M. R. AlRashidi and M. E. El-Hawary, "A survey of particle swarm optimization applications in electric power systems," *IEEE Trans. Evol. Comput.*, vol. 13, no. 4, pp. 913–918, Aug. 2009, doi: 10.1109/TEVC.2006.880326.

[36] A. Gálvez and A. Iglesias, "Efficient particle swarm optimization approach for data fitting with free knot -splines," *Comput.-Aided Des.*, vol. 43, no. 12, pp. 1683–1692, Dec. 2011, doi: 10.1016/j.cad.2011.07.010.

[37] R. H. Liang, S. R. Tsai, Y. T. Chen, and W. T. Tseng, "Optimal power flow by a fuzzy based hybrid particle swarm optimization approach," *Electr. Power Syst. Res.*, vol. 81, no. 7, pp. 1466–1474, Jul. 2011, doi: 10.1016/j.epsr.2011.02.011.

[38] X. Song, L. Tang, X. Lv, H. Fang, and H. Gu, "Application of particle swarm optimization to interpret Rayleigh wave dispersion curves," *J. Appl. Geophys.*, vol. 84, pp. 1–13, Sep. 2012, doi: 10.1016/j.jappgeo.2012.05.011.

[39] I. B. Aydilek, "A hybrid firefly and particle swarm optimization algorithm for computationally expensive numerical problems," *Appl. Soft Comput.*, vol. 66, pp. 232–249, May 2018, doi: 10.1016/j.asoc.2018.02.025.

[40] G. Ramarao and K. Chandrasekaran, "Use of PSO to determine lightning channel-base-current function parameters for standard severe negative first and subsequent return stroke approximation," *IET Sci., Meas. Technol.*, vol. 13, no. 1, pp. 42–52, Jan. 2019, doi: 10.1049/iet-smt.2018.5320.

[41] Z. A. A. Alyasseri, A. T. Khader, M. A. Al-Betar, A. K. Abasi, and S. N. Makhadmeh, "EEG signals denoising using optimal wavelet transform hybridized with efficient Metaheuristic methods," *IEEE Access*, vol. 8, pp. 10584–10605, 2020.

[42] S. N. Makhadmeh, A. T. Khader, M. A. Al-Betar, S. Naim, Z. A. A. Alyasseri, and A. K. Abasi, "Particle swarm optimization algorithm for power scheduling problem using smart battery," in *Proc. IEEE Jordan Int. Joint Conf. Electr. Eng. Inf. Technol. (JEEIT)*, Apr. 2019, pp. 672–677.
[43] M. N. Ab Wahab, S. Nefti-Meziani, and A. Atyabi, "A comprehensive review of swarm optimization algorithms," *PLoS ONE*, vol. 10, no. 5, May 2015, Art. no. e0122827, doi: 10.1371/journal.pone.0122827.
[44] K. Lee and J.-B. Park, "Application of particle swarm optimization to economic dispatch problem: Advantages and disadvantages," in *Proc. IEEE PES Power Syst. Conf. Expo.*, Oct. 2006, pp. 188–192, doi: 10.1109/PSCE.2006.296295.
[45] R. Poli, J. Kennedy, and T. Blackwell, "Particle swarm optimization an overview," *Swarm Intell.*, vol. 1, no. 1, pp. 33–57, 2007.
[46] D. Gong, L. Lu, and M. Li, "Robot path planning in uncertain environments based on particle swarm optimization," in *Proc. IEEE Congr. Evol. Comput.*, May 2009, pp. 2127–2134.
[47] Q. Bai, "Analysis of particle swarm optimization algorithm," *Comput. Inf. Sci.*, vol. 3, no. 1, pp. 180–184, Jan. 2010.
[48] F. Heidler and J. Cvetić, "A class of analytical functions to study the lightning effects associated with the current front," *Eur. Trans. Electr. Power*, vol. 12, no. 2, pp. 141–150, Mar. 2002, doi: 10.1002/etep.4450120209.
[49] D. A. Smith, X. M. Shao, D. N. Holden, C. T. Rhodes, M. Brook, P. R. Krehbiel, M. Stanley, W. Rison, and R. J. Thomas, "A distinct class of isolated intracloud lightning discharges and their associated radio emissions," *J. Geophys. Res., Atmos.*, vol. 104, no. D4, pp. 4189–4212, Feb. 1999, doi: 10.1029/1998JD200045.
[50] A. V. Gurevich and K. P. Zybin, "Runaway breakdown and the mysteries of lightning," *Phys. Today*, vol. 58, no. 5, pp. 37–43, May 2005, doi: 10.1063/1.1995746.
[51] S. S. Watson and T. C. Marshall, "Current propagation model for a narrow bipolar pulse," *Geophys. Res. Lett.*, vol. 34, no. 4, pp. 344–356, Feb. 2007, doi: 10.1029/2006GL027426.
[52] S. Karunarathne, T. C. Marshall, M. Stolzenburg, and N. Karunarathna, "Modeling initial breakdown pulses of CG lightning flashes," *J. Geophys. Res., Atmos.*, vol. 119, no. 14, pp. 9003–9019, Jul. 2014, doi: 10.1002/2014JD021553.
[53] S. Karunarathne, T. C. Marshall, M. Stolzenburg, and N. Karunarathna, "Electrostatic field changes and durations of narrow bipolar events: Electrostatic field changes of NBEs," *J. Geophys. Res. Atmos.*, vol. 121, no. 17, pp. 10161–10174, Sep. 2016, doi: 10.1002/2016JD024789.
[54] A. Nag and V. A. Rakov, "Compact intracloud lightning discharges: 1. Mechanism of electromagnetic radiation and modeling," *J. Geophys. Res.*, vol. 115, no. D20102, pp. 1–20, Oct. 2010, doi: 10.1029/2010JD014235.
[55] A. Nag and V. A. Rakov, "Compact intracloud lightning discharges: 2. Estimation of electrical parameters," *J. Geophys. Res.*, vol. 115, no. D20103, pp. 1–15, Oct. 2010, doi: 10.1029/2010JD014237.
[56] A. Nag and V. A. Rakov, "A unified engineering model of the first stroke in downward negative lightning," *J. Geophys. Res., Atmos.*, vol. 121, no. 5, pp. 2188–2204, Mar. 2016, doi: 10.1002/2015JD023777.

XIANGPENG FAN received the B.S. degree in atmospheric sciences from Lanzhou University, Lanzhou, China, in 2008, the M.Sc. degree in atmospheric physics from the Cold and Arid Regions Environment and Engineering Research Institute, Chinese Academy of Sciences, Lanzhou, in 2011, and the Ph.D. degree in atmospheric sciences from the Chinese Academy of Sciences, Beijing, China, in 2019.

He is currently an Associate Professor with the State Key Laboratory of Severe Weather, Chinese Academy of Meteorological Sciences. His research interests include lightning physics and lightning detection.

WEN YAO received the M.S. degree in atmospheric sounding from the Nanjing University of Information Science and Technology, Nanjing, China, in 2001.

She is currently a Professor with the Chinese Academy of Meteorological Sciences. Her research interests include the key technologies of meteorological observation instruments, the application of meteorological observational information, and severe weather forecasting.

YANG ZHANG received the Ph.D. degree in physical electronics from the Chinese Academy of Sciences in 2008.

He is currently a Professor with the State Key Laboratory of Severe Weather, Chinese Academy of Meteorological Science. His research interests include thunderstorm detection, lightning location, and lightning physics.

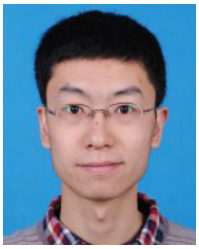

LIANGTAO XU received the B.S. degree in atmospheric sciences form Sun Yat-Sen University, in 2009, and the Ph.D. degree in meteorology from the Chinese Academy of Sciences, in 2015. In 2015, he joined the State Key Laboratory of Severe Weather, Chinese Academy of Meteorological Sciences, as an Assistant Professor.

YIJUN ZHANG received the B.Sc. degree in physics from Hebei Normal University, Hebei, China, in 1986, and the M.Sc. and Ph.D. degrees in atmospheric physics from the Cold and Arid Regions Environment and Engineering Research Institute, Chinese Academy of Sciences, Lanzhou, China, in 1989 and 1998, respectively.

He is a currently a Professor with the Department of Atmospheric and Oceanic Sciences/ Institute of Atmospheric Sciences, Fudan University, Shanghai, China. His research interests include atmospheric electricity, lightning physics, and thunderstorm electricity.

PAUL R. KREHBIEL received the B.Sc. and M.Sc. degrees in electrical engineering (physics option) from the Massachusetts Institute of Technology, in 1963 and 1966, respectively, and the Ph.D. degree in physics from the University of Manchester Institute of Science and Technology, in 1982. He is currently a semi-retired Professor of physics and a Lightning Researcher with the Langmuir Laboratory for Atmospheric Research, New Mexico Institute of Mining and Technology, Socorro, New Mexico.

DONG ZHENG received the B.S. degree in atmospheric sciences from Lanzhou University, in 2002, and the M.S. and Ph.D. degrees in atmospheric sciences from the Chinese Academy of Sciences, in 2005 and 2008, respectively.

Since 2016, he has been a Professor with the State Key Laboratory of Severe Weather, Chinese Academy of Meteorological Sciences. He is the author of more than 100 articles. His research interests include thunderstorm and lightning, severe weather, lightning detection, lightning physics, and lightning warning, and forecasting.

HENGYI LIU was born in Hebei, China, in 1981. He received the B.Sc. degree from Hebei University, Hebei, in 2004, and the Ph.D. degree from the Chinese Academy of Sciences, Beijing, China, in 2012.

He is currently an Associate Professor with the State Key Laboratory of Severe Weather, Chinese Academy of Meteorological Sciences. His research interests include lightning physics and lightning detection.

WEITAO LYU received the Ph.D. degree in atmospheric physics from the University of Science and Technology of China, Hefei, China, in 2003.

He is currently a Professor with the Chinese Academy of Meteorological Science, Beijing, China. His research interests include lightning physics, lightning detection, and lightning protection.

SHAODONG CHEN (Member, IEEE) received the B.Sc., M.Sc., and Ph.D. degrees in meteorological science from the Nanjing University of Information Science and Technology, Nanjing, China, in 2001, 2004, and 2010, respectively. He is currently a Research grade Senior Engineer with the Institute of Tropical and Marine Meteorology, CMA, Guangzhou. His research interests focus on lightning physics and lightning protection.

ZHENGSHUAI XIE received the bachelor's degree in atmospheric sounding from the Chengdu University of Information Technology, Chengdu, China, in 2017, where he is currently pursuing the master's degree in atmospheric physics.

His research interests include lighting physics and image correction.